Supporting Information for

Temporally Overlapped but Uncoupled Motions in Dihydrofolate Reductase Catalysis

C. Tony Liu,[†,‡] Lin Wang,[†,‡] Philip Hanoian,[†] Nina M. Goodey,[‖] Stephen J. Benkovic*[,†]

[†]Department of Chemistry, Pennsylvania State University, University Park, PA 16802, United States

[‖]Department of Chemistry and Biochemistry, Montclair State University, NJ 07043, United States

Corresponding author

*E-mail: sjb1@psu.edu. Phone: (814) 865-2882.

Preparation of DHFR

To enable labeling of DHFR at designated positions by the sulfhydryl group, native cysteines were removed from DHFR by using a gene that codes for the replacements C85A in helix αE and C152S in sheet βH (ΔCys-DHFR), as previously described.[1] Removal of these native cysteines does not significantly alter the catalytic properties of wild-type DHFR. All constructs involved were prepared from the mutant gene pET27b-bioseq-C85A-C152S-DHFR as described previously.[1] A quick change mutagenesis kit (Stratagene #200518) was used to generate the required DHFR mutations. The sequences of all constructs were verified by DNA sequencing at the Pennsylvania State University Huck Institute of the Life Sciences DNA Sequencing Facility using primers T7 and T7term primers.

To prepare all protein constructs, *E. coli* BL21(DE3) cells containing the appropriate plasmid were grown in LB medium containing 50 μg/mL kanamycin, and protein production was induced with 0.4 M isopropyl-β-D-galactopyranoside (IPTG). After induction, the temperature was reduced to 30 ºC, and the cells were allowed to grow for 14 hours and then centrifuged at 7000 rpm for 20 minutes at 4 ºC. The enzymes were then purified from the resulting cell pellets as previously described,[1] stored in -80 ºC, and the protein concentration was determined by measuring the absorbance at 280 nm and using the extinction coefficient $\varepsilon = 31{,}100\ cm^{-1}\ M^{-1}$. Fluorescence titration with methotrexate, which is a tight-binding inhibitor of DHFR, confirmed the protein concentration measurement.[2]

Attachment of fluorescent probes to DHFR

To prepare the labeled DHFR variants, the corresponding purified protein (40-100 mg) was diluted to 50 – 150 μM in 50 mM sodium phosphate, pH 7.2 with 10 % glycerol, and 1 mM TCEP at room temperature before a molar equivalent of Alexa Fluor 555 (1 mg/mL) was added. The reaction, shielded from light, was incubated at room temperature for 1-3 hours under gentle agitation. To improve the labeling specificity for the desired product, 0.4 mM NADPH (Sigma) was maintained in the reaction mixture to reduce the labeling efficiency at Residue 48 in the case of Construct A. And in the case of Construct B 4 M guanidine chloride was maintained to enhance the labeling efficiency at Residue 120. The labeled products was reconstituted by dialysis in 50 mM sodium phosphate, pH 7.2 with 10 % glycerol overnight and centrifuged to remove denatured proteins. Then the product mixture was loaded onto a column of 1 mL Source 15Q anion exchange resin for separation. The separated products were isolated and submitted to time-of-flight mass spectrometry with electrospray (+) ionization to determine their masses. Covalent attachment of Alexa Fluor 555 was by adding approximately 956 D to the mass of the unlabeled protein.

Mass spectrometry confirms the correct mass of the desired product but not the desired placement of the Alexa Fluor 555 probe. To confirm that the probe is attached to designated positions, chymotrypsin digestions were performed before tris tricine gel electrophoresis.[3] Labeled DHFR construct (10-50 μM) was incubated for 14 hours at 37 ºC in 0.2 M NH_4HCO_3 at pH 8.0 in the presence of 5 μg of chymotrypsin in a total volume of 40 μL. Single cysteine DHFR constructs labeled with Alexa Fluor 555 maleimide were used as controls. The Cypro red filter (Biorad) was used to image the gel so that only fragments with covalently attached Alexa

Fluor 555 dye were visible, allowing for comparison of the unknown, labeled fragment with control fragments.

To covalently attach the second dye, QSY 35 iodoacetamide (Invitrogen), the singly labeled intermediate was diluted to a concentration of 1 μM in 50 mM sodium phosphate at pH 7.2 with 10 % glycerol and 1 mM TCEP. A solution (1 mg/mL) of QSY 35 iodoacetamide was prepared in dimethyl sulfoxide, and 30 molar equivalents of dye to protein were added to the protein solution. The reaction was incubated at room temperature for 12-24 hours, covered from light. The reaction mixture was loaded onto approximately 3 mL of rinsed methotrexate-agarose resin (Sigma M0269), and the column was washed with 50-100 mL of 50 mM sodium phosphate at pH 7.2 with 10 % glycerol to remove any unfolded DHFR and free dye molecules. The DHFR construct was then eluted as described for the singly labeled constructs above. Complete labeling of ΔCys-DHFR with QSY 35 iodoacetamide was confirmed by determining the mass of the final product by time of flight mass spectrometry with electrospray (+ve) ionization. Addition of the QSY 35 probe added approximately an additional 561 D. A minimum of two separate batches of each construct and mutant were prepared and used to obtain the data below to rule out batch to batch variability.

Kinetic Experiments

All kinetic measurements were carried out following similar protocols described in previous studies.[4-5] In brief, the pre-steady state hydride transfer rates for the enzymatic reaction were determined by following NADPH disappearance (excitation at 290 nm/emission with 400 nm band pass filter) under single turnover conditions using an Applied Photophysics stopped-flow apparatus thermostatted at 25 ºC. The kinetic experiments were performed in MTEN buffer

(composed of 50mM MES, 25mM Tris, 25mM ethanolamine, and 100mM NaCl) adjusted to various pH (6.0, 7.0, or 8.5) values. One of the syringes in the stopped-flow analyzer was loaded with 5-10 μM enzyme, 1.25μM NADPH, 2mM DTT, and 50mM MTEM buffer (according to [MES]). The other syringe contained 200μM H_2F, 2mM DTT, and 50mM MTEM buffer. Upon mixing, the final concentrations of the individual species in the stopped-flow reaction chamber were halved (2.5-5 μM enzyme, 0.625μM NADPH, 100μM H_2F, 2mM DTT, and 50mM MTEM buffer). The emission vs. time traces were fitted to single exponential expressions to derive the kinetic rate constants (k_{hyd}). Parallel kinetic isotope effect experiments were performed using NADPD[6] instead of NADPH at pH 7.0. Steady-state turnover kinetics (k_{cat}) experiments were performed following similar experimental conditions as described above with the exceptions that the reaction progress was monitored at 340nm, and 200μM instead of 1.25 μM of NADPH was used (Table S1). Kinetic experiments were performed in at least duplicate runs with the averaged rate constants being used for further data analysis.

Conformational changes associated with fluorescence changes of the covalently bound probes were investigated under identical experimental conditions to those used to determine the hydride transfer rates as described above, and the detailed procedure has been reported in an earlier study.[5] The changes in the emission intensities of covalently attached Alexa Fluor 555 (excitation at 514 nm/550 nm band-pass filter) were recorded over time as it responded to the relative change to the QSY 35 iodoacetamide. The fluorescence intensity vs. time traces were fit to a single exponential expression to calculate the k_{FRET} values. It should be noted that in all cases control experiments showed no detectable fluorescence signal change for the apo-enzymes and binary complexes (DHFR:NADPH and DHFR:DHF) over 20 seconds when the protein samples were mixed with buffer solution and excited at the FRET acceptor excitation

wavelength. Furthermore, the singly labeled A145C ecDHFR with Alex Fluor 488 exhibited no change in the fluorescence intensity during the hydride transfer step. This suggests that despite being in a loop region, the probe on residue 145 does not experience significant deviation with regard to its local environment on the experimental time scale examined here. This also makes position 145 a good pivot point to probe the distance changes between residue 145 and any other residue as in constructs A and D (residue 148 was assumed to behave as residue 145 for the purpose of a 'static' reference point).

Table S1. Averaged turnover rate constants (k_{cat}) for the various ecDHFR constructs. ND = Not determined.

Construct (probe position)	k_{cat} at pH 7.0 (s^{-1})	k_{hyd} at pH 6.0 (s^{-1})	k_{hyd} at pH 8.5 (s^{-1})
WT ecDHFR[a]	12.5 ± 2.0	25	670
A (48-145)	10.5 ± 0.5	616 ± 50	58 ± 2.0
A (48-145) L54I mutation	6.0 ± 2.0	13.6 ± 0.3	0.23 ± 0.03
B (51-120)	ND	ND	ND
C (101-148)	ND	ND	ND
D (120-145)	16.1 ± 1.2	ND	2.0 ± 0.5
E (17-37)[b]	11.4 ± 1.7	483 ± 80	9.4
E (17-37)[b] G121V mutation	6.0 ± 0.6	10 ± 1	0.50 ± 0.05

[a]Data from reference (4).

[b] Data from reference (5).

The L51I mutant of construct A and the G121V mutant of construct E yielded turnover rate constants (k_{cat}; Table S1) that are similar to the hydride transfer rate constants (k_{hyd}; Table 2). Thus the k_{cat} and the k_{hyd} values for those two mutants are essentially the same within experimental uncertainty, especially since they were measured under different conditions. This suggests that the L51I and the G121V mutations are perturbative enough to the catalyzed hydride transfer reaction that at pH 7.0 the rate limiting step of the catalytic cycle is the hydride transfer step.

Table S2 lists the C_α-C_α distances between the residues used for the FRET pairs both in the Michaelis-Menten complex (PDB ID 7DFR; closed conformation modeled by DHFR:FOL:$NADP^+$) and the initial product complex (PDB ID 1RC4; occluded conformation, modeled by DHFR:ddTHF:$NADP^+$).[7] In all cases, increased fluorescence signals were detected between all FRET pairs when dihydrofolate was mixed with the E:NADPH complex, suggesting enhanced FRET efficiency in the product state compared to the reactant state. Since the structural data in Table S2 indicates a subtle increase in the distance between the residue pairs, the increased FRET efficiency is likely due to changes in the relative geometric orientations between the probes.

Table S2. List of C_α-C_α distances between the specific residue pairs determined from crystal structure data[7].

Construct	Protein components	Residue pairs	C_α-C_α distance Closed conformation (E:FOL:$NADP^+$)	C_α-C_α distance Occluded conformation (E:ddTHF:$NADP^+$)

A	GH loop	48 – 145	28.1 Å	29.6 Å
B	G51 loop	51 – 120	23.5 Å	24.1 Å
C	GH loop	101 – 148	28.4 Å	28.5 Å
D	FG relatives to GH loops	120 – 145	23.3 Å	24.8 Å
E	Met20 loop	17 – 37	29.2 Å	22.3 Å

Empirical Valence Bond Molecular Dynamics Simulations

We performed classical MD simulations of wild-type *E. coli* DHFR using a two-state empirical valence bond (EVB) potential to examine the thermally averaged distance changes along the collective reaction coordinate between the residues labeled with fluorescent probes in the FRET experiments. In this framework, the reaction coordinate is defined as the difference in energy between the two valence bond states in the EVB potential. The simulations were performed using the mapping potential approach for 19 values of the coupling parameter lambda.[8-9] For each mapping potential, three independent trajectories were propagated for 100 ps of equilibration and 500 ps of production. The data from all of the independent trajectories were combined using the weighted histogram analysis method (WHAM)[10] to generate the free energy profile along the collective reaction coordinate with a total of 28.5 ns total sampling. The two parameters in the EVB potential associated with the coupling between the two valence bond states and their relative energies were fit to reproduce the experimental free energies of activation and reaction. Configurations sampled from the MD trajectories at intervals of 1 ps were weighted according to the probabilities determined using the WHAM to obtain thermally averaged inter-C_α distances along the collective reaction coordinate. The value of each thermally averaged distance was extracted at the reactant and product free energy minima and at the

transition state free energy maximum along the collective reaction coordinate. These MD simulations were performed using a modified version of the DLPROTEIN program.[11] The complete methodological details of these MD simulations have been published previously.[12]

Using empirical valence bond (EVB) molecular dynamics (MD) simulations to model the hydride transfer reaction in wild-type ecDHFR, we calculated the equilibrium thermally averaged C_α-C_α distance changes occurring during the hydride transfer reaction in wild-type ecDHFR for the residue pairs that were fluorescently labeled in constructs A to E. As shown in Table S3, the thermally averaged C_α-C_α distances between the labeled residues do not change significantly as the system evolves from the reactant state (RS) to the transition state (TS) to the product state (PS) along the collective reaction coordinate associated with the hydride transfer reaction. We also surveyed the thermally averaged C_α-C_α distance change between selected residues (17, 51, 120, and 145; ones used in the FRET experiments) and all other residues in the protein (Figure S1). These residues were selected to probe conformational changes in four regions of interest in the enzyme: the Met20 loop, G51 loop, GH loop, and FG loop. As shown in Figure S1, these thermally averaged C_α-C_α distance changes across the chemical step are subtle and sub-angstrom in magnitude. The computed C_α-C_α distance changes typically indicate a greater degree of distance change between the TS (red lines in Figure S1) and PS (blue lines in Figure S1) than between the RS and TS. It should be noted that distance changes in the range of 0.1 angstrom should be considered to be numerically insignificant. Moreover, the Met20 loop remains in the closed configuration during the MD trajectories. It is possible that the FRET data report on the changes associated with the conversion from the closed conformation (DHFR Michaelis-Menten complex) to the occluded conformation (initial product complex),[7,13] and the changes observed in the FRET experiments are not captured by the simulations performed here.

However, both experimental and computational data presented here did not find conformational changes that are directly linked to the hydride transfer reaction.

Table S3. Thermally averaged distances from EVB MD simulations of the hydride transfer reaction.

Construct	Protein Components	Residue Pairs	Reactant State	Transition State	Product State
A	GH loop	48 – 145	28.8 Å	28.9 Å	29.1 Å
B	G51 loop	51 – 120	23.2 Å	23.2 Å	23.1 Å
C	GH loop	101 – 148	29.0 Å	28.8 Å	29.2 Å
D	FG relatives to GH loops	120 – 145	23.0 Å	23.0 Å	23.2 Å
E	Met20 loop	17 – 37	29.5 Å	29.5 Å	29.6 Å

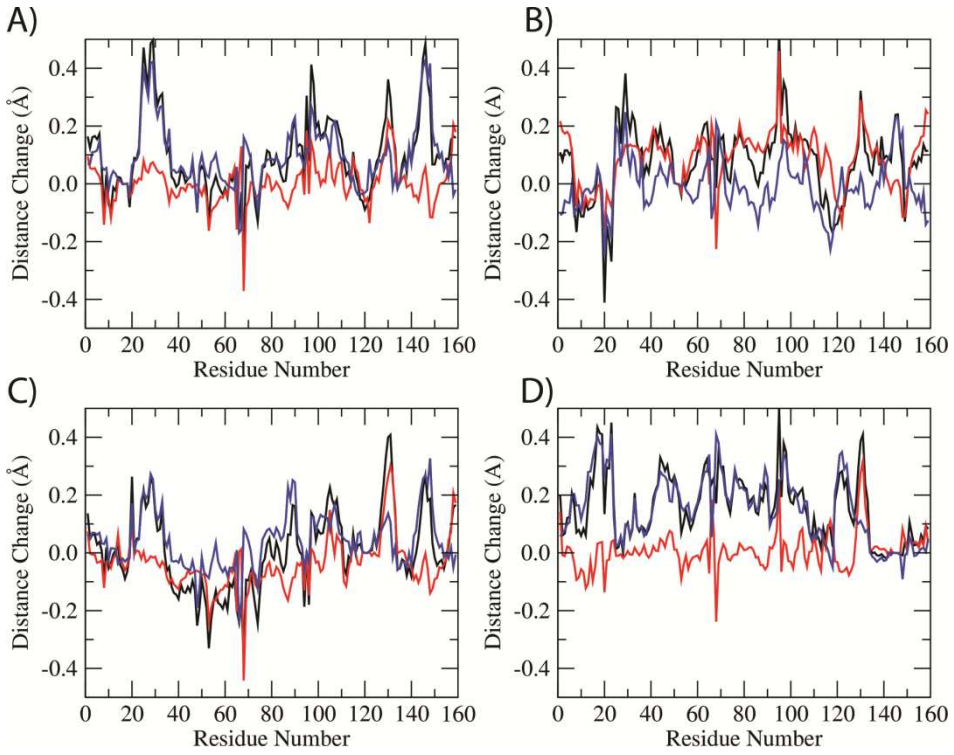

Figure S1. Calculated equilibrium C_α-C_α distance changes between all residues and residues A) E17, B) G51, C) E120, and D) A145 across the reaction coordinate of the wild-type ecDHFR catalyzed hydride transfer reaction (red RS → TS, blue TS → PS, and black RS → PS).

References

1. Agarwal, P. K., Billeter, S. R., Rajagopalan, P. T., Benkovic, S. J., and Hammes-Schiffer, S. (2002) *Proc. Natl. Acad. Sci. U.S.A 99*, 2794-2799.
2. Miller, G. P., Wahnon, D. C., and Benkovic, S. J. (2001) *Biochemistry 40*, 867-875.
3. Schagger, H., and von Jagow, G. (1987) *Anal Biochem 166*, 368-379.
4. Fierke, C. A., Johnson, K. A., and Benkovic, S. J. (1987) *Biochemistry 26*, 4085-4092.
5. Antikainen, N. M., Smiley, R. D., Benkovic, S. J., and Hammes, G. G. (2005) *Biochemistry 44*, 16835-16843.
6. Jeong, S. S., and Gready, J. E. (1994) *Anal Biochem 221*, 273-277.
7. Sawaya, M. R., and Kraut, J. (1997) *Biochemistry 36*, 586-603.
8. Warshel, A. (1991) *Computer Modeling of Chemical Reactions in Enzymes and Solutions*, John Wiley & Sons, Inc., New York.
9. Agarwal, P. K., Billeter, S. R., and Hammes-Schiffer, S. (2002) *J Phys Chem B 106*, 3283-3293.
10. Kumar, S., Bouzida, D., Swendsen, R. H., Kollman, P. A., and Rosenberg, J. M. (1992) *J Comput Chem 13*, 1011-1021.
11. Melchionna, S., and Cozzini, S. (2001) DLPROTEIN: Molecular Dynamics Software Package for Macrosmolecules 2.1 ed., INFM UDrSISSA, Triste, Italy.
12. Liu, C. T., Hanoian, P., French, J. B., Pringle, T. H., Hammes-Schiffer, S., and Benkovic, S. J. (2013) *Proc. Natl. Acad. Sci. U.S.A 110*, 10159-10164.
13. Boehr, D. D., McElheny, D., Dyson, H. J., and Wright, P. E. (2006) *Science 313*, 1638-1642.